

Rare B D decays in SUSY without R-parity

Tai-fu Feng

Institute of Theoretical Physics, Academia Sinica, P.O. Box 2735, Beijing 100080, P.R. China

Email: fengtf@itp.ac.cn

Abstract

We perform the complete computation of the contributions to $b \rightarrow s^+ e^- e^-$, $b \rightarrow s^+ e^- e^+ e^-$ in the SUSY with bilinear R-parity violation model. We compare the results with the evaluations in the SM. From those processes, we can get some constraint on the parameters in this model.

12.60.Jv, 13.10.+q, 14.80.Ly, 13.20.Jf, 12.15.Ff

arXiv:hep-ph/9808379v1 21 Aug 1998

I. INTRODUCTION

It is being increasingly realized by those engaged in the search for the supersymmetry (SUSY) [1] that the principle of R-parity conservation, assumed to be sacrosanct in the prevalent search strategies, is not inviolable in practice. The R-parity of a particle is defined as $R = (-1)^{L+3B+2S}$, and can be violated if either baryon (B) or lepton (L) number is not conserved in nature, a fact perfectly compatible with the non observation of proton decay. This is because, whereas the violation of B or L, taken singly, is inadmissible in the Standard Model (SM) where all the elementary baryons and leptons are fermions, the SUSY version of the SM allows it by virtue of the scalar quarks and leptons that are part of the particle spectrum.

Under R-parity violation the phenomenology changes considerably [2;3], the most important consequence is that the lightest supersymmetric particle (LSP) can decay now. However, the way in which R-parity can be violated is not unique. Different types of R-parity violating interaction terms can be written down, leading to different observable predictions. In addition, R-parity can be violated spontaneously, instead of explicitly, whence another class of interesting effects are expected [4]. If the phenomenology of R-parity breaking has to be understood, and the consequent modifications in the current search strategies have to be effectively implemented, then it is quite important to explore the full implication of each possible R-breaking scheme.

The R-conserving part of the minimal supersymmetric standard model (MSSM) is specified by the superpotential W_{MSSM} is given by:

$$W_{MSSM} = \mu_{ij} \hat{H}_i^1 \hat{H}_j^2 + \mu_{ij} \hat{L}^{IJ} \hat{H}_i^1 \hat{L}_j^I \hat{R}^J + \mu_{ij} d^{IJ} \hat{H}_i^1 \hat{Q}_j^I \hat{D}^J + \mu_{ij} u^{IJ} \hat{H}_i^2 \hat{Q}_j^I \hat{U}^J \quad (1)$$

where $I; J = 1; 2; 3$ are generation indices, $i; j = 1; 2$ are SU(2) indices, and μ is a completely antisymmetric 2×2 matrix, with $\mu_{12} = 1$. The symbol "hat" over each letter indicates a superfield, $\hat{Q}^I; \hat{L}^I; \hat{H}^1$, and \hat{H}^2 being SU(2) doublets with hyper-charges $\frac{1}{3}; -1; -1$; and 1 respectively, $\hat{U}; \hat{D}$, and \hat{R} being SU(2) singlets with hyper-charges $\frac{4}{3}; \frac{2}{3}$, and 2 respectively. The couplings $u^{IJ}; d^{IJ}$, and \hat{L}^{IJ} are 3×3 Yukawa matrices, and μ is parameter with units of mass. If now lepton number terms interactions are incorporated, the superpotential takes the form [5]:

$$W = W_{MSSM} + W_L \quad (2)$$

with $W_L = \mu_{ij} \hat{L}_i^I \hat{L}_j^I$ and μ_I is the parameter with units of mass.

The soft SUSY-breaking terms are:

$$\begin{aligned} L_{\text{soft}} = & m_{H_1}^2 H_1^1 H_1^1 + m_{H_2}^2 H_2^1 H_2^1 + (m_L^I)^2 \hat{L}_i^I \hat{L}_i^I \\ & (m_R^I)^2 \hat{R}^I \hat{R}^I + (m_Q^I)^2 \hat{Q}_i^I \hat{Q}_i^I + (m_D^I)^2 \hat{D}^I \hat{D}^I \\ & (m_U^I)^2 \hat{U}^I \hat{U}^I + (m_{1B}^I + m_{2A}^I) \\ & + m_G^a \hat{G}_a + h.c.) + (B \mu_{ij} \hat{H}_i^1 \hat{H}_j^2 + B_{1I} \mu_{ij} \hat{H}_i^2 \hat{L}_j^I \\ & + \mu_{ij} \hat{L}_s^I H_1^1 \hat{L}_j^I \hat{R}^I + \mu_{ij} \hat{L}_s^I H_1^1 \hat{Q}_j^I \hat{D}^I \\ & + \mu_{ij} \hat{L}_s^I H_1^2 \hat{Q}_j^I \hat{U}^I + h.c.) \end{aligned} \quad (3)$$

where $m_{H_1}, m_{H_2}, m_L^I, m_R^I, m_Q^I, m_D^I$; and m_U^I stand for the mass of the scalar fields while m_1, m_2, m_3 denote the mass of the SU(3) SU(2) U(1) gauginos \tilde{a}_G, \tilde{a}_A and \tilde{b}_B, B and B_1 are free parameters with units of mass.

The W_L and lepton-number breaking terms in L_{soft} give a viable agent for R-parity breaking. It is particularly interesting for the fact that it can trigger a mixing between neutralinos and neutrinos as well as between charginos and charged leptons, resulting in observable effects. For the \tilde{a}_G can reach a large value (such as $j^3 j \sim 500 \text{ GeV}$)^[5], the mixing between charginos and charged leptons may give an important contribution to the rare B decays such as $b \rightarrow s + \tilde{\nu}_\tau, b \rightarrow s e^+ e^-, b \rightarrow s e e$.

On the other hand, flavor-changing neutral current (FCNC) processes have constantly played a major role in the development of electroweak theories. FCNC studies have found kaon physics as their best research ground so far. However, the achievements in B-physics make B-mesons the new challenging frontier in the study of FCNC phenomena. At least some of the rare B-processes which are induced by the FCNC transitions $b \rightarrow s$ and $b \rightarrow d$ are within the reach of present machines. Needless to say, the test of such rare B-processes presents a probe of the validity of crucial ingredients of the Standard Model (SM) and, possibly of the existence of new physics beyond the SM at the low energy scale.

The $b \rightarrow s + \tilde{\nu}_\tau$ and $b \rightarrow s e^+ e^-$ in the SM are analyzed in Ref [6;7]. The SM prediction for the branching ratio (BR) of the inclusive decay $b \rightarrow s + \tilde{\nu}_\tau$, once the large QCD corrections are included^[6], is a few times 10^{-4} . As for the semileptonic $b \rightarrow s e^+ e^-$ decay, the QCD-corrected SM prediction for its BR is about 10^{-6} ^[7].

The FCNC rare B-processes have been widely analyzed as a potential probe for extensions of the SM implying new physics at the TeV scale. In the model with Two Higgs Doublets (THDM) and no tree level FCNC, the rare B decays and $B_d - \bar{B}_d$ mixing are computed in Ref [8;9]. As for left-right symmetric models, the simplest choice of taking the CKM mixing angles in the right-handed sector equal to the corresponding left-handed ones (manifest or pseudo-manifest left-right symmetry) does not give any appreciable effects with respect to the SM estimates of rare B-processes^[10]. Analogous results are obtained in the general case if no fine tunings of the parameters are allowed^[11].

The FCNC in the supersymmetry with R-parity has been discussed widely in Ref [12], Ref [13{15], FCNC in SUSY without R-parity has been discussed in Ref [16], the review of FCNC in the supersymmetry can be found in Ref [17].

This paper is organized as follows. In sect.2, we give a description of the general structure of the supersymmetry with bilinear R-parity violation. In sect.3, we provide the complete analyses to $b \rightarrow s + \tilde{\nu}_\tau, b \rightarrow s e^+ e^-, b \rightarrow s e e$ in the SUSY with bilinear R-parity violation. In sect.4, we perform a numerical analysis of those processes and we compare them with the predictions of the SM. For completeness, we provided the analytic expressions for Feynman integrals which one encounters in the evaluation of the amplitudes listed in sect.3 in appendix A. A systematic notation for the relevant Feynman rules involving R-parity breaking terms are introduced in appendix B. For simplicity, we neglect the generation mixing of slepton and squark in the following analyses.

II. MINIMAL SUSY MODEL WITH BILINEAR R-PARITY VIOLATION

As that has been stated before, we consider a superpotential of the form:^[5]

$$\begin{aligned}
W = & \kappa_{ij} \hat{H}_i^1 \hat{H}_j^2 + \lambda^I \kappa_{ij} \hat{H}_i^1 \hat{L}_j^I \hat{R}^I + u^I (\hat{H}_1^2 C^{JI} \hat{Q}_2^J \\
& \hat{H}_2^2 \hat{Q}_1^I) \hat{U}^I + d^I (\hat{H}_1^1 \hat{Q}_2^I + \hat{H}_2^1 C^{IJ} \hat{Q}_1^J) \hat{D}^I \\
& + \lambda^I \kappa_{ij} \hat{H}_i^2 \hat{L}_j^I
\end{aligned} \tag{4}$$

where the C is the Kobayashi-Maskawa matrix. The soft breaking sector has the form :

$$\begin{aligned}
L_{\text{soft}} = & m_{H_1}^2 H_1^1 H_1^1 + m_{H_2}^2 H_1^2 H_1^2 + (m_L^I)^2 \bar{L}_i^I \bar{L}_i^I + (m_R^I)^2 \bar{R}^I \bar{R}^I \\
& (m_Q^I)^2 \bar{Q}_i^I \bar{Q}_i^I + (m_D^I)^2 \bar{D}^I \bar{D}^I + (m_U^I)^2 \bar{U}^I \bar{U}^I + (m_{1B})^2 \bar{B} \\
& + m_{2A}^2 \bar{A} + m_{3A}^2 \bar{A} + m_{3G}^2 \bar{G} + h.c.) + f_B \kappa_{ij} H_1^1 H_j^2 + B_1 \kappa_{ij} H_1^2 \bar{L}_j^I \\
& + \kappa_{ij}^I H_1^1 \bar{L}_j^I \bar{R}^I + d_s^I (H_1^1 \bar{Q}_2^I + C^{IK} H_2^1 \bar{Q}_1^K) \bar{D}^I \\
& + u_s^I (C^{KI} H_1^2 \bar{Q}_2^I + H_2^2 \bar{Q}_1^I) \bar{U}^I + h.c.
\end{aligned} \tag{5}$$

For simplicity we take from now on $\mu = \nu = 0$, in this way, that only $B-L$ lepton number is violated. The electroweak symmetry is broken when the two Higgs doublets H_1 and H_2 , and the ν -sneutrino acquire vacuum expectation values (VEVs):

$$H_1^1 = \frac{1}{\sqrt{2}} \begin{pmatrix} 0 \\ v_1 + i' v_1^0 \end{pmatrix} \tag{6}$$

$$H_1^2 = \frac{1}{\sqrt{2}} \begin{pmatrix} v_1^0 \\ 0 \\ v_2 + i' v_2^0 \end{pmatrix} \tag{7}$$

$$\bar{\nu}_3 = \frac{1}{\sqrt{2}} \begin{pmatrix} 0 \\ v_3 + i' v_3^0 \\ \sim \end{pmatrix} \tag{8}$$

Note that the gauge bosons W and Z_0 acquire masses given by $m_W^2 = \frac{1}{4} g^2 v^2$ and $m_Z^2 = \frac{1}{4} (g^2 + g'^2) v^2$, where $v^2 = v_1^2 + v_2^2 + v_3^2$ and g, g' are coupling constants of $SU(2)$ and $U(1)$. We introduce the following notation in spherical coordinates [3]:

$$\begin{aligned}
v_1 &= v \sin \theta \cos \phi \\
v_2 &= v \sin \theta \sin \phi \\
v_3 &= v \cos \theta
\end{aligned} \tag{9}$$

which preserves the MSSM definition $\tan \beta = \frac{v_2}{v_1}$. The angle θ equals to $\frac{\pi}{2}$ in the MSSM limit and the massless neutral Goldstone boson can be written as:

$$G^0 = \sin \theta \cos \phi G_1^0 + \sin \theta \sin \phi G_2^0 + \cos \theta G_3^0 \tag{10}$$

In the model with bilinear R -parity violation, the charged Higgs bosons mix with the left and right staus. In the original basis, where $\phi_c = (H_2^1; H_1^2; \tilde{\nu}_L; \tilde{\nu}_R)$, the scalar potential contains the following mass term :

$$L_m^C = \sum_c y_c^2 \phi_c^2 \tag{11}$$

$$(Z^+)^T M_f Z = \begin{pmatrix} 0 & & & 1 \\ m & 0 & 0 & \\ 0 & m_{\tilde{1}} & 0 & \\ 0 & 0 & m_{\tilde{2}} & \end{pmatrix} \begin{matrix} B \\ B \\ C \\ A \end{matrix} \quad (17)$$

The unitary matrices Z^+ and Z are not uniquely specified – by changing their relative phases and the order of the eigenvalues. It is possible to choose m ; $m_{\tilde{1}}$ positive and (if necessary) $m_{\tilde{2}} > m_{\tilde{1}} > m$.

III. COMPLETE ANALYZE THE RARE B-PROCESSES IN THE SUSY WITH BILINEAR R-PARITY VIOLATION

Because we neglect the generation mixing of sleptons and squarks, there is no contribution of gluino and neutralino when we compute the rare processes such as $b \rightarrow s + \gamma$, $b \rightarrow s + e^+ e^-$ and $b \rightarrow s + e^- e^+$ at one loop level. In order to give the effective lagrangian for $b \rightarrow s e^+ e^-$ and $b \rightarrow s e^- e^+$, we should calculate the bsZ coupling and bs coupling at first.

A. bsZ, bs coupling and box diagrams in the SUSY with bilinear R-parity violation

We follow the method that was used by Ref [18]. In the $U(1)$ Higgs Feynman gauge, the one-loop diagrams for the induced bsZ coupling are shown in Fig. 1. The diagrams Fig. 1 (a), Fig. 1 (b) and Fig. 1 (c) represent the SM's contribution of the $b \rightarrow s$ transition. In each group, the first two diagrams (except for Fig. 1 (c)) are selfenergy part. Since the weak current is not conserved, we only need to expect a non-vanishing zeroth-order contribution in the momentum q . The induced bsZ coupling take the form

$$\Gamma_Z^{(i)} = s P_L b^{(i)} \quad (18)$$

where $i = a, b, c, d, e$. The $\Gamma_Z^{(i)}$ can be written as:

$$\begin{aligned} (a) = & \frac{e^3}{(4)^2 \sin^3 \theta_W \cos \theta_W} C_{ts} C_{tb} \left(\left(\frac{1}{2} - \frac{1}{3} \sin^2 \theta_W \right) (2f_2^{(0)}(x_{tw})) \right. \\ & 4f_{3b}^{(1)}(x_{tw}) + \left. \left(\frac{1}{4} - \frac{1}{3} \sin^2 \theta_W \right) f_{3b}^{(1)}(x_{tw}) \right. \\ & \left. \frac{2}{3} \sin^2 \theta_W x_{tw} f_{3b}^{(0)}(x_{tw}) + \frac{3}{2} \cos^2 \theta_W f_{3a}^{(1)}(x_{tw}) \right) \end{aligned} \quad (19)$$

$$\begin{aligned} (b) = & \frac{e^3}{(4)^2 \sin^3 \theta_W \cos \theta_W} C_{ts} C_{tb} \left(\left(\frac{1}{2} - \frac{1}{3} \sin^2 \theta_W \right) \frac{x_{tw}}{2} (f_2^{(0)}(x_{tw}) - 2f_{3b}^{(1)}(x_{tw})) + \right. \\ & \left. \frac{x_{tw}}{2} \left(\left(\frac{1}{2} - \frac{2}{3} \sin^2 \theta_W \right) x_{tw} f_{3b}^{(0)}(x_{tw}) + \frac{1}{3} \sin^2 \theta_W f_{3b}^{(1)}(x_{tw}) \right) + \right. \\ & \left. \frac{x_{tw}}{8} (\cos^2 \theta_W - \sin^2 \theta_W) f_{3a}^{(1)}(x_{tw}) \right) \end{aligned} \quad (20)$$

$$(c) = \frac{e^3}{(4)^2 \sin^3 \theta_W \cos \theta_W} C_{ts} C_{tb} \frac{P_-}{2 \sin^2 \theta_W} x_{tw} f_{3a}^{(0)}(x_{tw}) \quad (21)$$

$$\begin{aligned}
(d) = & \frac{e^3}{(4)^2 \sin^3 \omega \cos \omega} C_{ts} C_{tb} \left(\frac{1}{2} \frac{1}{3} \sin^2 \omega \right) \frac{x_{tw}}{2 \sin^2 \nu \sin^2} X^4 Z_H^{2i} Z_H^{2i} (f_2^{(0)}(x_{ts_i})) \\
& 2f_{3b}^{(1)}(x_{ts_i}) + \frac{x_{tw}}{2 \sin^2 \nu \sin^2} X^4 Z_H^{2i} Z_H^{2i} \left(\frac{1}{2} \frac{2}{3} \sin^2 \omega \right) x_{ts_i} f_{3b}^{(0)}(x_{ts_i}) + \\
& \frac{1}{3} \sin^2 \omega f_{3b}^{(0)}(x_{ts_i}) \frac{x_{tw}}{8 \sin \nu \sin} X^4 X^4 Z_H^{2i} Z_H^{2j} ((\cos^2 \omega \\
& \sin^2 \omega)_{ij} Z_H^{4i} Z_H^{4j}) f_{3c}^{(1)}(x_{ts_i}; x_{s_j s_i})) \quad (22)
\end{aligned}$$

$$\begin{aligned}
(e) = & \frac{e^3}{(4)^2 \sin^3 \omega \cos \omega} C_{ts} C_{tb} \left(\sum_{i=1}^2 \sum_{j=1}^2 j (Z_T^{1i} Z_{1j}^+ + \frac{Z_T^{2i} Z_{2j}^+}{2M_W \sin \nu \sin}) \right) \frac{1}{2} \\
& \frac{1}{3} \sin^2 \omega (f_2^{(0)}(x_{\sim_j t_i}) - 2f_{3b}^{(1)}(x_{\sim_j t_i})) + \sum_{i,j=1}^2 X^2 X^3 (Z_T^{1i} Z_{1j}^+ + \frac{m_t Z_T^{2i} Z_{2j}^+}{2M_W \sin \nu \sin}) \\
& (Z_T^{11} Z_{1j}^+ + \frac{m_t Z_T^{21} Z_{2j}^+}{2M_W \sin \nu \sin}) \left(\frac{1}{4} Z_T^{11} Z_T^{1i} \frac{1}{3} \sin^2 \omega \right) f_{3c}^{(0)}(x_{\sim_j t_i}; x_{t_i t_i}) + \\
& \sum_{i,j=1}^2 X^3 X^2 \frac{1}{2} (Z_T^{11} Z_{1j}^+ + \frac{m_t Z_T^{21} Z_{2j}^+}{2M_W \sin \nu \sin}) (Z_T^{11} Z_{1j}^+ + \frac{m_t Z_T^{21} Z_{2j}^+}{2M_W \sin \nu \sin}) \\
& ((Z_{1j} Z_{1i} + 2 \cos^2 \omega) \frac{1}{2} f_{3c}^{(1)}(x_{\sim_i t_i}; x_{\sim_j t_i}) + x_{\sim_i t_i} x_{\sim_j t_i} (Z_{1j}^+ Z_{1i}^+ \\
& + 2 \cos^2 \omega) f_{3c}^{(0)}(x_{\sim_i t_i}; x_{\sim_j t_i})) \quad (23)
\end{aligned}$$

where $s_{i=1,2,3,4} = G, H, \sim_1, \sim_2$ and $x = \frac{m^2}{M^2}$

Notice that the ultraviolet divergences cancel separately for each of those equation. In obtaining the form shown, the unitary property of Z_H, Z_T, Z^+ and Z have been used, together with the unitarity of the Kobayashi-Maskawa matrix.

The computation of the photon exchange contribution is somewhat more involved and requires the calculation of the induced bs coupling up to second order in the external momentum. The diagrams need to be computed are those of Fig. 1 with Z being replaced by γ . The induced bs coupling takes the form :

$$(F_1^{(i)}) = s (F_1^{(i)}(q^2) - q \not{\epsilon}) P_L + F_2^{(i)} \not{\epsilon} (m_s P_L + m_b P_R) \quad (24)$$

where $i = a; b; c; d; e$ and

$$\begin{aligned}
F_1^{(a)} = & \frac{1}{(4)^2} \frac{e^3}{\sin^2 \omega} C_{tb} C_{ts} \frac{1}{M_W^2} \left(\frac{1}{9} f_{5d}^{(2)}(x_{tw}) - \frac{2}{3} f_{4c}^{(1)}(x_{tw}) + \right. \\
& \left. \frac{1}{2} f_{3a}^{(0)}(x_{tw}) + \frac{1}{2} f_{4b}^{(1)}(x_{tw}) - \frac{3}{2} f_{4a}^{(1)}(x_{tw}) + \right. \\
& \left. \frac{4}{3} f_{5a}^{(2)}(x_{tw}) - \frac{1}{3} f_{5b}^{(2)}(x_{tw}) \right) \quad (25)
\end{aligned}$$

$$F_2^{(a)} = \frac{1}{(4)^2} \frac{e^3}{\sin^2 \omega} C_{tb} C_{ts} \frac{1}{M_W^2} \left(\frac{2}{3} f_{3b}^{(0)}(x_{tw}) - f_{4c}^{(1)}(x_{tw}) + \right)$$

$$\begin{aligned}
& \frac{1}{3} f_{5d}^{(2)}(\mathbf{x}_{tw}) + \frac{1}{2} f_{3a}^{(0)}(\mathbf{x}_{tw}) - \frac{3}{2} f_{4b}^{(1)}(\mathbf{x}_{tw}) \\
& \frac{1}{4} f_{4a}^{(1)}(\mathbf{x}_{tw}) + \frac{1}{3} f_{5c}^{(2)}(\mathbf{x}_{tw}) + \frac{1}{3} f_{5b}^{(2)}(\mathbf{x}_{tw}) + \frac{2}{9} \left(\frac{\ln \mathbf{x}_{tw}}{\mathbf{x}_{tw}} \right. \\
& \left. + \ln \frac{m_c^2}{M_W^2} + f\left(\frac{q^2}{m_b^2}\right) \right)
\end{aligned} \tag{26}$$

$$\begin{aligned}
F_1^{(b)} = & \frac{1}{(4)^2} \frac{e^3}{\sin^2 w} C_{tb} C_{ts} \frac{1}{M_W^2} \left(\frac{\mathbf{x}_{tw}}{18} f_{5d}^{(2)}(\mathbf{x}_{tw}) - \frac{\mathbf{x}_{tw}}{12} f_{5c}^{(2)}(\mathbf{x}_{tw}) + \right. \\
& \left. \frac{\mathbf{x}_{tw}}{12} f_{5b}^{(2)}(\mathbf{x}_{tw}) \right)
\end{aligned} \tag{27}$$

$$\begin{aligned}
F_2^{(b)} = & \frac{1}{(4)^2} \frac{e^3}{\sin^2 w} C_{tb} C_{ts} \frac{1}{M_W^2} \left(\frac{\mathbf{x}_{tw}}{2} f_{4c}^{(1)}(\mathbf{x}_{tw}) - \frac{\mathbf{x}_{tw}}{6} f_{5d}^{(2)}(\mathbf{x}_{tw}) + \right. \\
& \frac{3\mathbf{x}_{tw}}{8} f_{4b}^{(1)}(\mathbf{x}_{tw}) - \frac{1}{6} f_{5c}^{(2)}(\mathbf{x}_{tw}) \\
& \left. \frac{1}{12} f_{5b}^{(2)}(\mathbf{x}_{tw}) \right)
\end{aligned} \tag{28}$$

$$F_1^{(c)} = \frac{1}{(4)^2} \frac{e^3}{\sin^2 w} C_{tb} C_{ts} \frac{\mathbf{x}_{tw}}{M_W^2} f_{5a}^{(2)}(\mathbf{x}_{tw}) \tag{29}$$

$$F_2^{(c)} = \frac{1}{(4)^2} \frac{e^3}{\sin^2 w} C_{tb} C_{ts} \frac{1}{4M_W^2} f_{4a}^{(1)}(\mathbf{x}_{tw}) \tag{30}$$

$$\begin{aligned}
F_1^{(d)} = & \frac{1}{(4)^2} \frac{e^3}{\sin^2 w} C_{tb} C_{ts} \frac{X^4}{i=2} \frac{Z_H^{2i} Z_H^{2i}}{6M_W^2 \sin^2 w \sin^2} \left(\frac{1}{3} f_{5d}^{(2)}(\mathbf{x}_{ts_i}) \right. \\
& \left. \frac{1}{2} f_{5c}^{(2)}(\mathbf{x}_{ts_i}) + \frac{1}{2} f_{5b}^{(2)}(\mathbf{x}_{ts_i}) \right)
\end{aligned} \tag{31}$$

$$\begin{aligned}
F_2^{(d)} = & \frac{1}{(4)^2} \frac{e^3}{\sin^2 w} C_{tb} C_{ts} \frac{X^4}{i=2} \left(\frac{\mathbf{x}_{ts_i}}{6M_W^2 \sin^2 w} \left(\frac{Z_H^{2i} Z_H^{2i}}{\sin^2} + 2 \frac{Z_H^{1i} Z_H^{2i}}{\sin \cos} \right) f_{4c}^{(1)}(\mathbf{x}_{ts_i}) \right. \\
& \frac{Z_H^{2i} Z_H^{2i}}{\sin^2} f_{5d}^{(2)}(\mathbf{x}_{ts_i}) + \frac{\mathbf{x}_{ts_i}}{2M_W^2 \sin^2 v} \left(\frac{Z_H^{2i} Z_H^{2i}}{4\sin^2} f_{4b}^{(1)}(\mathbf{x}_{ts_i}) + \right. \\
& \frac{Z_H^{1i} Z_H^{2i}}{2\sin \cos} f_{4b}^{(1)}(\mathbf{x}_{ts_i}) - \frac{Z_H^{2i} Z_H^{2i}}{3\sin^2} f_{5c}^{(2)}(\mathbf{x}_{ts_i}) \\
& \left. \left. \frac{Z_H^{2i} Z_H^{2i}}{6\sin^2} f_{5b}^{(2)}(\mathbf{x}_{ts_i}) \right) \right)
\end{aligned} \tag{32}$$

$$\begin{aligned}
F_1^{(e)} = & \frac{1}{(4)^2} \frac{e^3}{\sin^2 w} C_{tb} C_{ts} \frac{X^3}{i=1; j=1} \frac{1}{m_{\tilde{t}_i}^2} \mathcal{Z}_T^{1i} \mathcal{Z}_{1;j}^+ \frac{m_t Z_T^{2i} Z_j^+}{2M_W \sin v \sin} f \left(\frac{2}{9} f_{5a}^{(2)}(\mathbf{x}_{\tilde{t}_j \tilde{t}_i}) + \right. \\
& \left. \frac{1}{6} f_{5d}^{(2)}(\mathbf{x}_{\tilde{t}_j \tilde{t}_i}) \right)
\end{aligned} \tag{33}$$

$$\begin{aligned}
F_2^{(e)} = & \frac{1}{(4)^2} \frac{e^3}{\sin^2 w} C_{tb} C_{ts} \sum_{i=1;2} \sum_{j=1}^3 \frac{1}{m_{t_i}^2} (Z_T^{1i} Z_{1j}^+ - \frac{m_t Z_T^{2i} Z_{2j}^+}{2M_W \sin v \sin}) f_2 \left(\frac{1}{2} f_{4c}^{(1)}(\mathbf{x}_{\sim_j t_i}) + \right. \\
& \left. \frac{1}{2} f_{5d}^{(2)}(\mathbf{x}_{\sim_j t_i}) - \frac{2}{3} f_{4b}^{(1)}(\mathbf{x}_{\sim_j t_i}) + \frac{2}{9} f_{5c}^{(2)}(\mathbf{x}_{\sim_j t_i}) \right. \\
& \left. - \frac{1}{18} f_{5b}^{(2)}(\mathbf{x}_{\sim_j t_i}) \right) - \frac{1}{2} (Z_T^{1i} Z_{1j}^+ + \frac{m_t Z_T^{2i} Z_{2j}^+}{2M_W \sin v \sin}) \frac{Z_T^{1i} Z_{2j} m_{\sim_j}}{2M_W \sin v \cos} \\
& (f_{4c}^{(1)}(\mathbf{x}_{\sim_j t_i}) + \frac{2}{3} f_{4b}^{(1)}(\mathbf{x}_{\sim_j t_i})) \quad (34)
\end{aligned}$$

The function $f(s)$ is defined as:

$$f(s) = \begin{cases} \frac{2}{3} \frac{z}{s} + \frac{8}{3} \frac{z}{s} \geq 2(1 + \frac{z}{2s}) \frac{1}{s} \tan^{-1} \left[\frac{z}{s} \sqrt{1 - \frac{z}{s}} \right]^{-1}; & \text{if } s < z; \\ \frac{2}{3} \frac{z}{s} + \frac{8}{3} \frac{z}{s} \leq (1 + \frac{z}{2s}) \frac{1}{s} \left[\ln \frac{1 + \sqrt{1 - \frac{z}{s}}}{1 - \sqrt{1 - \frac{z}{s}}} \right]^{-1}; & \text{if } s > z \end{cases} \quad (35)$$

where $z = \frac{4m_c^2}{m_b^2}$ and $f(0) = 1$. The other functions are given in appendix A.

The box-diagrams that contribute to the $b \rightarrow s e^+ e^-$ are shown in Fig. 2, The effective lagrangian takes the form :

$$A_i^{\text{box}}(s, P_L b)(e, P_L e) \quad (36)$$

with

$$A_a^{\text{box}} = \frac{1}{(4)^2} \frac{e^4}{4\sin^4 w} C_{ts} C_{tb} \frac{1}{M_W^2} f_{4d}^{(1)}(\mathbf{x}_{tw}; 0) \quad (37)$$

$$\begin{aligned}
A_b^{\text{box}} = & \frac{1}{(4)^2} \frac{e^4}{4\sin^4 w} C_{ts} C_{tb} \sum_{i,j=1}^3 \sum_{l=1}^3 \frac{1}{m_{t_i}^2} Z_{1j}^+ Z_{li}^+ (Z_T^{1l} Z_{1j}^+ + \frac{m_t Z_T^{2l} Z_{2i}^+}{2M_W \sin v \sin}) \\
& (Z_T^{1l} Z_{1j}^+ + \frac{m_t Z_T^{2l} Z_{2i}^+}{2M_W \sin v \sin}) f_{4e}^{(1)}(\mathbf{x}_{\sim_j t_i}; \mathbf{x}_{\sim_i t_l}; \mathbf{x}_{\sim_e t_l}) \quad (38)
\end{aligned}$$

As for $b \rightarrow s e e$, it is analogous to the case of $b \rightarrow s e^+ e^-$. The box diagrams that contribute to the $b \rightarrow s e e$ are given in Fig. 3. The effective lagrangian takes the form :

$$B_i^{\text{box}}(s, P_L b)(e, P_L e) \quad (39)$$

with

$$B_a^{\text{box}} = \frac{1}{(4)^2} \frac{e^4}{4\sin^4 w} C_{ts} C_{tb} \frac{1}{M_W^2} f_{4d}^{(1)}(\mathbf{x}_{eW}; \mathbf{x}_{tw}) \quad (40)$$

$$\begin{aligned}
B_b^{\text{box}} = & \frac{1}{(4)^2} \frac{e^4}{4\sin^4 w} C_{ts} C_{tb} \frac{1}{m_{t_i}^2} \sum_{h=1;2} \sum_{i,j=1;2} \sum_{l=1;2}^3 Z_E^{1h} Z_E^{1h} Z_{li} Z_{1j} (Z_T^{1l} Z_{1i}^+ + \frac{m_t Z_T^{2l} Z_{2i}^+}{2M_W \sin v \sin}) \\
& (Z_T^{1l} Z_{1i}^+ + \frac{m_t Z_T^{2l} Z_{2i}^+}{2M_W \sin v \sin}) f_{4e}^{(1)}(\mathbf{x}_{\sim_i t_l}; \mathbf{x}_{\sim_j t_l}; \mathbf{x}_{\sim_e t_l}) \quad (41)
\end{aligned}$$

B. The width of $b \rightarrow s + \gamma$ in the SUSY with bilinear R-parity violation

The total amplitude of the decay $b \rightarrow s + \gamma$ can therefore be written as:

$$A_{\text{tot}}(b \rightarrow s + \gamma) = F_2 O_{LR} \quad (42)$$

with F_2 is the sum of Eq. (26), Eq. (28), Eq. (30), Eq. (32), Eq. (34). Where $O_{LR} = m_b \text{ seq } P_{Rb}$ and the contribution of $O_{RL} = m_s \text{ seq } P_{Lb}$ is neglected since it is of $O(\frac{m_s}{m_b})$.

By denoting the total amplitude at a scale μ as $F_2(\mu)$, the QCD-corrected amplitude at the scale of the process ($\mu = m_b$) is then given by: [15]

$$F_2(m_b) = \frac{16}{23} f F_2(M_W) + F_2^0 \left[\frac{116}{135} \left(\frac{10}{23} - 1 \right) + \frac{58}{189} \left(\frac{28}{23} - 1 \right) \right] g \quad (43)$$

where

$$F_2^0 = \frac{1}{(4\pi)^2} \frac{e^3}{\sin^3 \theta_W} C_{tb} C_{ts} \frac{1}{M_W^2} \quad (44)$$

The property $C_{cs} C_{cb} = C_{ts} C_{tb}$ for the 3×3 CKM matrix has been used in the previous equation. The inclusive width for the $b \rightarrow s + \gamma$ decay is finally given by:

$$\Gamma(b \rightarrow s + \gamma) = \frac{m_b^5}{16} F_2(m_b)^2 \quad (45)$$

Where we have neglected the phase-space factors of order $O(\frac{m_s^2}{m_b^2})$. We calculate the corresponding branching ratio as in Ref [19] by making use of the semileptonic decay $b \rightarrow c e \bar{\nu}_e$, one gets:

$$BR(b \rightarrow s + \gamma) = \frac{\Gamma(b \rightarrow s + \gamma)}{\Gamma(b \rightarrow c e \bar{\nu}_e)} BR(b \rightarrow c e \bar{\nu}_e) \quad (46)$$

where for $BR(b \rightarrow c e \bar{\nu}_e)$ we use the averaged experimental value 0.11 [20]. The QCD-corrected width for the semileptonic decay $b \rightarrow c e \bar{\nu}_e$ is [21]

$$\Gamma(b \rightarrow c e \bar{\nu}_e) = \frac{G_F^2 m_b^5}{192 \cdot 3} \left(\frac{m_c}{m_b}; 0; 0 \right) \mathcal{F}_{bc}^2 f_1 \left(\frac{2}{3} \frac{m_b}{m_c} \right) f \left(\frac{m_c}{m_b}; 0; 0 \right) g \quad (47)$$

where the phase-space factor is 0.447 and $f(\frac{m_c}{m_b}; 0; 0) = 2.41$, G_F is the coupling constant for the four fermion coupling.

C. The width of $b \rightarrow s e^+ e^-$ in the SUSY with bilinear R-parity violation

This decay has been often considered the benchmark of charmless b-decays with strange particles in the final state. We will provide below the amplitude for $b \rightarrow s e^+ e^-$ including QCD effects. In what follows, the same conventions as in the previous decay have been adopted.

We begin by considering the diagrams which induce the effective flavor-changing coupling of the photon to quarks (photon⁰ penguins). They are given by the diagrams shown in Fig. 1 with a lepton line attached to the photon propagator. We consider separately the monopole (LL) and

dipole(LR) form factor, which are related to different effective operators.

(i)photon penguins(LL component)

$$A_{\text{tot}}^{iLL}(b \rightarrow se^+e^-) = eF_1 O_{LLV} \quad (48)$$

where $O_{LLV} = (s \rightarrow P_L b)(e \rightarrow e)$ and F_1 is the sum of Eq. (25), Eq. (27), Eq. (29), Eq. (31), Eq. (33).

(ii)Photon penguins(LR component)

$$A_{\text{tot}}^{iLR}(b \rightarrow se^+e^-) = eF_2 O_{LRV} \quad (49)$$

with F_2 is the sum of Eq. (26), Eq. (28), Eq. (30), Eq. (32), Eq. (34) and the operator O_{LRV} is defined as:

$$O_{LRV} = m_b \frac{1}{q^2} (s \rightarrow P_R b)(e \rightarrow e)$$

(iii) Z^0 -penguins. The process $b \rightarrow se^+e^-$ is also induced by the effective FC coupling of the Z^0 to quarks. The total amplitude coming from the Z^0 -penguins can be expressed as:

$$A_{\text{tot}}^Z(b \rightarrow se^+e^-) = \frac{e}{M_Z^2 \sin \theta_w \cos \theta_w} \zeta \left(\frac{1}{2} O_{LLL} + \sin^2 \theta_w O_{LLV} \right) \quad (50)$$

where the new operator O_{LLL} is given as

$$O_{LLL} = (s \rightarrow P_L b)(e \rightarrow P_L e)$$

and $\zeta = \sum_z^{(i)}$ is the sum of Eq. (19), Eq. (20), Eq. (21), Eq. (22) and Eq. (23).

(iv)Box diagrams. The relevant contributions are given in Eq. (37), Eq. (38).

In order to implement the QCD corrections, let us rewrite the total amplitude at the M_W scale as:

$$A_{\text{tot}}^{(b \rightarrow se^+e^-)}(M_W) = A_{LLV}(M_W) O_{LLV} + A_{LRV}(M_W) O_{LRV} + A_{LLL}(M_W) O_{LLL} \quad (51)$$

with:

$$\begin{aligned} A_{LLV}(M_W) &= F_1 + \sin^2 \theta_w A^Z \\ A_{LRV}(M_W) &= F_2 \\ A_{LLL}(M_W) &= A^Z + 2 + (A_a^{\text{box}} + A_b^{\text{box}}) \end{aligned} \quad (52)$$

Renormalization at the m_b -scale then leads to: [21]

$$\begin{aligned} A_{LLV}(m_b) &= A_{LLV}(M_W) + \sin^2 \theta_w A^Z(M_W) + A_0^0 \frac{4}{s(M_W)} f \frac{8}{87} \left[1 - \frac{29}{23} \right] \\ &\quad + \frac{4}{33} \left[1 - \frac{11}{23} g \right] + \frac{4}{9} A_0^0 \left[\ln \left(\frac{m_c^2}{m_b^2} \right) + f(s) \right] \left[2 - \frac{6}{23} \right] \end{aligned} \quad (53)$$

$$A_{LRV}(m_b) = \frac{16}{23} f A_{RV}(M_W) + A_0^0 \left[\frac{116}{135} \left(\frac{10}{23} - 1 \right) + \frac{58}{189} \left(\frac{28}{23} - 1 \right) \right] g \quad (54)$$

$$A_{LLL}(m_b) = A_{LLL}(M_W) \quad (55)$$

where $A_0^0 = F_2^0 \frac{P}{4}$, and F_2^0 have been defined in Eq. (44).

The differential decay rate is then given by: [5]

$$\begin{aligned} \frac{d}{ds} = \frac{m_b^5}{1536} & \frac{4}{3} (1 - s^2) f \left(\frac{1}{2} + s \right) [A_{LLV}^2 + A_{LLL}^2 + A_{LLV}^2] \\ & + \left(1 + \frac{2}{s} \right) A_{LRV}^2 - 3 \text{Re}[(2A_{LLV} + A_{LLL})A_{LRV}] g \end{aligned} \quad (56)$$

where $s = \frac{q^2}{m_b^2}$

D. The width of $b \rightarrow s e e$ in the SUSY with bilinear R-parity violation

The transition $b \rightarrow s e e$ is induced by Z^0 -penguins and box diagrams, which, at the leading order, lead to the same effective operator. The peculiarity of this process is that it is not affected by the QCD renormalization. This is simply understood by noticing that the current $(s \rightarrow p_L b)$ is conserved in the limit of vanishing quark masses. Conserved currents have canonical dimensions and no divergent counterterms arise. This ultraviolet behavior is not spoiled by consideration of finite quark masses. [5]

The original electroweak sensitivity to the top mass is therefore preserved. On the other hand, the experimental search for this rare B-transition is understandably much harder than for the previous semileptonic decay.

For the e-neutrino type, we obtain the following results (Under our presumes, the e-neutrino is not mixing with neutralino.):

$$A_{\text{tot}}(b \rightarrow s e e) = A_{0LLL} \quad (57)$$

where $A = A^Z + B_a^{\text{box}} + B_b^{\text{box}}$ with $A^Z = \frac{e}{\sin_w \cos_w} Z$ and $B_{a,b}^{\text{box}}$ is given in Eq. (40) and Eq. (41). The decay rate for the e-neutrino is then given by

$$(b \rightarrow s e e) = \frac{m_b^5}{1536} \frac{4}{3} A_{LLL}^2 \quad (58)$$

IV. NUMERICAL RESULTS

In the previous section, we have taken the parameters independently at the weak scale. As we know, there are many free parameters in the general SUSY model. For simplicity, we take the constraint as follows at weak scale in the numerical evaluation:

$$\begin{aligned} \frac{l_{(I=3)}}{l_{s(I=3)}} = \frac{d_{(I=3)}}{d_{s(I=3)}} = \frac{u_{(I=3)}}{u_{s(I=3)}} = \frac{l_{(I=2)}}{l_{s(I=2)}} = \dots = \frac{u_{(I=1)}}{u_{s(I=1)}}; \\ B = \frac{l_{(I=3)}}{l_{s(I=3)}} - 1; \\ m_{H_1}^2 = m_{H_2}^2 = (m_L^{I=3})^2 = (m_R^{I=3})^2 = (m_Q^{I=3})^2 = (m_U^{I=3})^2 = \\ (m_D^{I=3})^2 = (m_L^{I=2})^2 = \dots = (m_U^{I=1})^2 = (m_D^{I=1})^2; \\ m_3 = m_2 = m_1 = M_{\frac{1}{2}} \end{aligned} \quad (59)$$

Those constraint combine with the equation that the VEV⁰s of the Higgs and the $\tilde{\nu}_\tau$ -sneutrino satisfy, they leave ve free parameters in this model, we can choose them as $\tan \beta$, $\tan \alpha$, μ , $M_{\frac{1}{2}}$, and M_3 . As for the other parameters that used in the numerical evaluation, we take $\frac{1}{4} = \frac{e^2}{4}$, $\frac{1}{137.03}$, $m_s(M_W) = 0.118$, $m_e = 0.511\text{M ev}$, $m_\tau = 1.777\text{G ev}$, $M_Z = 91.187\text{G ev}$, $M_W = 80.330\text{G ev}$, $m_t = 179\text{G ev}$, $m_c = 1.3\text{G ev}$ and $m_b = 4.3\text{G ev}$

In order to find out the allowed region in the parameter space, one has to take a number of constraints into account. First, we note that μ , $M_{\frac{1}{2}}$, and M_3 are the four free parameters that enter into the charginos and neutralino mass matrices. The strongest constraint on them follows from the fact that the $\tilde{\nu}_\tau$ mass has been experimentally measured [20], therefore, for any combination of the μ , $M_{\frac{1}{2}}$, and M_3 , the lowest eigenvalue of Eq. (16) should agree with m_τ . Also,

$\tilde{\nu}_\tau$ has a laboratory upper limit of 24M ev on its mass. Those two restrictions, together with the Higgs mass matrices' positive-definite condition, constrain the parameter space in a severe manner. Furthermore, we are interested in relatively light charginos, and that is why we take $M_{\frac{1}{2}} = 500$ G ev and $\mu = 500$ G ev.

We open our discussion by considering the radiative decay $b \rightarrow s + \gamma$. When we take constraint Eq. (59), the value of μ must be less than zero from the Higgs mass matrices' positive-definite condition, this is the reason that we take the parameter $\mu < 0$. In Fig. 4, Fig. 5 and Fig. 6 we plot the branching ratio of $b \rightarrow s + \gamma$ as a function μ under some different value of $\tan \beta$ and $\tan \alpha$. (The dependence on the remnant SUSY parameter such as μ , $M_{\frac{1}{2}}$ is represented by the vertical width of the band.) We see that positive interference with the different sources of SUSY contributions produces a moderate enhancement over the QCD-corrected SM prediction (horizontal solid line). Furthermore, the contribution of R-breaking terms is the same order as the usual R-parity conserving terms' contribution. The present experimental bound on the inclusive transition is $\text{BR}(b \rightarrow s + \gamma) < 1.2 \times 10^{-3}$, so we can get some constraint on the parameter space under our presume. If we release the Eq. (59), the case is very involved.

We turn now to the semileptonic FCNC decay $b \rightarrow s + e^+ e^-$ and $b \rightarrow s + e e$. In the SM, the QCD-corrected $\text{BR}(b \rightarrow s + e^+ e^-)$ is about 9×10^{-6} . The addition of the one-loop contributions where SUSY particles are present modify the prediction up to about ten times the SM's prediction as it can be gathered from Fig. 7, Fig. 8 and Fig. 9. The dominant contribution is come from the R-breaking terms. Analogous considerations hold for $b \rightarrow s + e e$ (Fig. 10, Fig. 11 and Fig. 12). The R-breaking terms can have an appreciable effects for the $b \rightarrow s + e e$. This is the main difference between the BRpV model and the usual SUSY model with R-parity.

In summary, as a simple extension of the MSSM which introduce R-parity violation, the R-breaking terms in BRpV model can give an appreciable effects for the rare B-processes. From the present experimental bound on those processes, we can get some constraint on the parameters in this model.

APPENDIX A : VARIOUS FUNCTION

We collect in this appendix the various function appearing in the processes computed in the text. The one-variable function obtained from the penguin diagrams are:

$$f_2^{(0)}(x) = \frac{x}{1-x} \ln x \quad (\text{A1})$$

$$f_{3a}^{(0)}(x) = \frac{1}{1-x} f_1 + \frac{x}{1-x} \ln xg \quad (\text{A2})$$

$$f_{3b}^{(0)}(x) = \frac{1}{1-x} f_1 + \frac{1}{1-x} \ln x g \quad (A 3)$$

$$f_{3a}^{(1)}(x) = \frac{2 \ln x}{1-x} + \ln x \left[\frac{\ln x}{(1-x)^2} - \frac{1}{(1-x)} \right] \quad (A 4)$$

$$f_{3b}^{(1)}(x) = \frac{2x \ln x}{1-x} \ln x + \frac{x^2 \ln x}{(1-x)^2} + \frac{x}{(1-x)} \quad (A 5)$$

$$f_{4a}^{(1)}(x) = \frac{1}{(x-1)} \left[\frac{1}{2} + \frac{x}{x-1} - \frac{x^2}{(x-1)^2} \ln x \right] \quad (A 6)$$

$$f_{4b}^{(1)}(x) = \frac{2}{(x-1)} \left[\frac{1}{2} - \frac{x}{x-1} - \frac{x}{(x-1)^2} \ln x \right] \quad (A 7)$$

$$f_{4c}^{(1)}(x) = \frac{1}{(x-1)} \left[\frac{1}{2} - \frac{1}{x-1} - \frac{1}{(x-1)^2} \ln x \right] \quad (A 8)$$

$$f_{5a}^{(2)}(x) = \frac{1}{3(x-1)} + \frac{x}{2(x-1)^2} + \frac{x^2}{(x-1)^3} - \frac{x^3}{(x-1)^4} \ln x \quad (A 9)$$

$$f_{5b}^{(2)}(x) = \frac{5}{2(x-1)} - \frac{3x}{2(x-1)^2} + \frac{3x^2}{(x-1)^3} - \frac{3x^2}{(x-1)^4} \ln x \quad (A 10)$$

$$f_{5c}^{(2)}(x) = \frac{1}{2(x-1)} + \frac{3x}{2(x-1)^2} + \frac{3}{(x-1)^3} - \frac{3x}{(x-1)^4} \ln x \quad (A 11)$$

$$f_{5d}^{(2)}(x) = \frac{1}{3(x-1)} + \frac{1}{2(x-1)^2} - \frac{1}{(x-1)^3} + \frac{1}{(x-1)^4} \ln x \quad (A 12)$$

The two- and three-variable functions obtained from penguin and box diagrams are:

$$f_{3c}^{(0)}(x; y) = \frac{1}{x} \left[\frac{x}{y} \frac{\ln x}{x-1} - \frac{y}{y-1} \ln y \right] \quad (A 13)$$

$$f_{3c}^{(1)}(x; y) = \frac{1}{2(x-y)} \left[\frac{x^2}{x-1} \ln x - \frac{y^2}{y-1} \ln y \right] \quad (A 14)$$

$$f_{4d}^{(1)}(x; y) = \frac{1}{x-y} \left[\frac{x^2}{(x-1)^2} \ln x - \frac{1}{x-1} (x-y) \right] \quad (A 15)$$

$$f_{4e}^{(1)}(x; y; z) = \frac{1}{x} \frac{1}{y} \frac{1}{x-z} \left[\frac{x^2}{(x-1)} \ln x - \frac{3x}{2} (x-z) - (x-y) g \right] \quad (A 16)$$

APPENDIX B : THE RELEVANT FEYNMAN RULE IN THE SUSY WITH
BILINEAR R-PARITY VIOLATION

We report in this appendix the relevant Feynman rules, involving supersymmetric particles, used in the calculation of the various processes.

It is first convenient to introduce the mixing matrices relative to the scalar-quark sector. We denote with $\mathcal{Q}_{L,R}^I$ the squark current eigenstates (where $I = 1;2;3$ is the generation label and $q = u;d$), and with $\mathcal{q}_{1,2}^I$ the corresponding mass eigenstates of the I -th generation (we neglect the generation-mixing of the scalar-quark and scalar-lepton). The 2×2 mixing matrices Z_{q^I} are defined by:

$$\begin{aligned}\mathcal{Q}_L^I &= Z_{q^I}^{1i} \mathcal{q}_i^I \\ \mathcal{Q}_R^I &= Z_{q^I}^{2i} \mathcal{q}_i^I\end{aligned}\quad (\text{B1})$$

Similar, the 2×2 mixing matrices Z_E is defined as:

$$\begin{aligned}\mathbf{e}_L &= Z_E^{1i} \mathbf{e}_i^I \\ \mathbf{e}_R &= Z_E^{2i} \mathbf{e}_i^I\end{aligned}\quad (\text{B2})$$

with $\mathbf{e}_{L,R}$ are the selectron's current eigenstates and $\mathbf{e}_{1,2}$ are the corresponding mass eigenstates. The S_i , up quark and down quark coupling can be written as (Fig. 13):

$$i\left[\frac{em_d^I}{2M_W \sin_W \sin_\nu \cos} Z_H^{1i} P_L + \frac{em_u^J}{2M_W \sin_W \sin_\nu \sin} Z_H^{2i} P_R\right] \mathcal{C}_{IJ} \quad (\text{B3})$$

The coupling of down quark, up scalar quark and chargino (Fig. 14):

$$i\left[\left(\frac{e}{\sin_W} Z_{u^I}^{1i} Z_{1j}^+ + \frac{em_u^J}{2M_W \sin_W \sin_\nu \sin} Z_{u^I}^{2i} Z_{2j}^+\right) P_L + \frac{em_d^I}{2M_W \sin_W \sin_\nu \cos} Z_{u^J}^{1i} Z_{2j} P_R\right] \mathcal{C}_{IJ} \quad (\text{B4})$$

The coupling of up quark, down scalar quark and chargino (Fig. 15):

$$i\left[\left(\frac{e}{\sin_W} Z_{d^I}^{1i} Z_{1j}^+ + \frac{em_d^I}{2M_W \sin_W \sin_\nu \cos} Z_{d^I}^{2i} Z_{2j}\right) P_L + \frac{em_u^J}{2M_W \sin_W \sin_\nu \sin} Z_{d^I}^{1i} Z_{2j}^+ P_R\right] \mathcal{C}_{IJ} \quad (\text{B5})$$

The coupling of Z^0 and s_i are (Fig. 16):

$$i \frac{e}{2 \sin_W \cos_W} [(\cos^2_W - \sin^2_W) i_j Z_H^{4i} Z_H^{4j}] (\not{p} + \not{k}) \quad (\text{B6})$$

where $s_i = (G; H; \tilde{\gamma}_1; \tilde{\gamma}_2); i = 1;2;3;4$. The matrices $Z_H; Z$ have been defined as before.

REFERENCES

- [1] For reviews see, for example, H.P. Nilles, *Phys. Rep.* 110, 1 (1984); H.E. Haber and G.L. Cane, *ibid* 117,75 (1985).
- [2] See, for example, R. Barbieri and L. Hall, *Phys. Lett. B* 238, 86 (1990); V. Barger et al. *Phys. Rev. D* 44, 1629 (1991); R. Godbole, P. Roy and X. Tata, *Nucl. Phys. B* 401, 67 (1993).
- [3] S. Roy and B.M. Mukhopadhyaya, *Phys. Rev. D* 55, 7020 (1997); R. Hemping, *Nucl. Phys. B* 478, 3 (1996); B. de Carlos, P.L. White, *Phys. Rev. D* 55, 4222 (1997).
- [4] C.S. Aulakh and R.N. Mohapatra, *Phys. Lett.* 119B, 136 (1982); A. Masiero and T. Valle, *Phys. Lett. B* 251, 273 (1990); G. Giudice et al, *Nucl. Phys. B* 396, 243 (1993); I. Umemura and K. Yamamoto, *ibid*, B 423, 405 (1994).
- [5] M.A. Diaz, J.C. Romao and J.W.F. Valle, *hep-ph/9706315*.
- [6] N.G. Deshpande, P.Lo, J. Trampetic, G. Eilam and P. Singer, *Phys. Rev. Lett.* 59, 183 (1987); B. Grinstein, R. Springer and M. Wise, *Phys. Lett. B* 202, 138 (1988), *Nucl. Phys. B* 339, 269 (1990); R. Grijanis, P. J. O'Donnell, M. Sutherland and H. Navelet, *Phys. Lett. B* 213, 355 (1988).
- [7] N.G. Deshpande and J. Trampetic, *Phys. Rev. Lett.* 60, 2583 (1988); C.A. Dominguez, N. Paver and Riazuddin, *Z. Phys. C* 48, 55 (1990).
- [8] W.-S. Hou and R.S. Willey, *Nucl. Phys. B* 236, 54 (1989).
- [9] A.J. Buras, P. Krawczyk, M.E. Lautenbacher and C. Salazar, *Nucl. Phys. B* 337, 284 (1990); V. Barger, J.L. Hewett and R.J.N. Phillips, *Phys. Rev. D* 41, 3421 (1990); J.F. Gunion and B. Grzadkowski, *Phys. Lett. B* 243, 301 (1990).
- [10] D. Colicchio, G. Costa, G.L. Fogli, J.H. Kim and A. Masiero, *Phys. Rev. D* 40, 1477 (1989).
- [11] D. London and D. Wyler, *Phys. Lett. B* 232, 503 (1989).
- [12] F. Zwimer, *Phys. Lett. B* 132, 103 (1983); J.-M. Gerard, W. Grimus, Anitava Raychaudhuri and G. Zoupanos, *Phys. Lett. B* 140, 349 (1984).
- [13] M. Dugan, B. Grinstein and L. Hall, *Nucl. Phys. B* 255, 413 (1985); L.J. Hall, V.A. Kostelecky and S. Raby, *Nucl. Phys. B* 267, 415 (1986).
- [14] J.S. Hagelin, S. Kelley and T. Tanaka, *Nucl. Phys. B* 415, 293 (1994); F. Gabbiani, E. Gabrielli, A. Masiero and L. Silvestrini, *Nucl. Phys. B* 477, 321 (1996).
- [15] S. Bertolini, F. Borzumati, A. Masiero and G. Ridol, *Nucl. Phys. B* 353, 591 (1991); F. Gabbiani and A. Masiero, *Nucl. Phys. B* 322, 235 (1989); S. Bertolini and J. Matias, *hep-ph/9709330*.
- [16] R. Barbieri and A. Masiero, *Nucl. Phys. B* 267, 679 (1986).
- [17] A. Masiero and L. Silvestrini, *hep-ph/9711401*; A. Masiero and L. Silvestrini, *hep-ph/9709244*.
- [18] T. Inami and C.S. Lim, *Prog. of. Theo. Phys.* V 65, 297 (1981); M.K. Gaillard, B.W. Lee and R.E. Shrock, *Phys. Rev. D* 13, 2674 (1976); E.B. Bogomolny, V.A. Vainstein and M.A. Shifman, *Yadarn. Fiz.* 23, 825 (1976) [*Soviet J. Nucl. Phys.* 23, 935 (1976)]; V.V. Flambaum, *Yadarn. Fiz.* 22, 661 (1975) [*Soviet J. Nucl. Phys.* 22, 340 (1976)]; M.B. Voloshin, *Yadarn. Fiz.* 24, 810 (1976) [*Soviet J. Nucl. Phys.* 24, 422 (1976)].
- [19] S. Bertolini, F. Borzumati and A. Masiero, *Phys. Rev. Lett.* 59, 180 (1987).
- [20] Particle Data Group. R.M. Barnett et al, *Phys. Rev. D* 54, 1 (1996).
- [21] N. Cabibbo and L. Maiani, *Phys. Lett. B* 79, 109 (1978); J.L. Cortes, X.Y. Pham and A. Tounsi, *Phys. Rev. D* 25, 188 (1982); G.L. Fogli, *Phys. Rev. D* 28, 1153 (1983).
- [22] B. Grinstein, M.J. Savage and M.B. Wise, *Nucl. Phys. B* 319, 271 (1989).

FIGURES

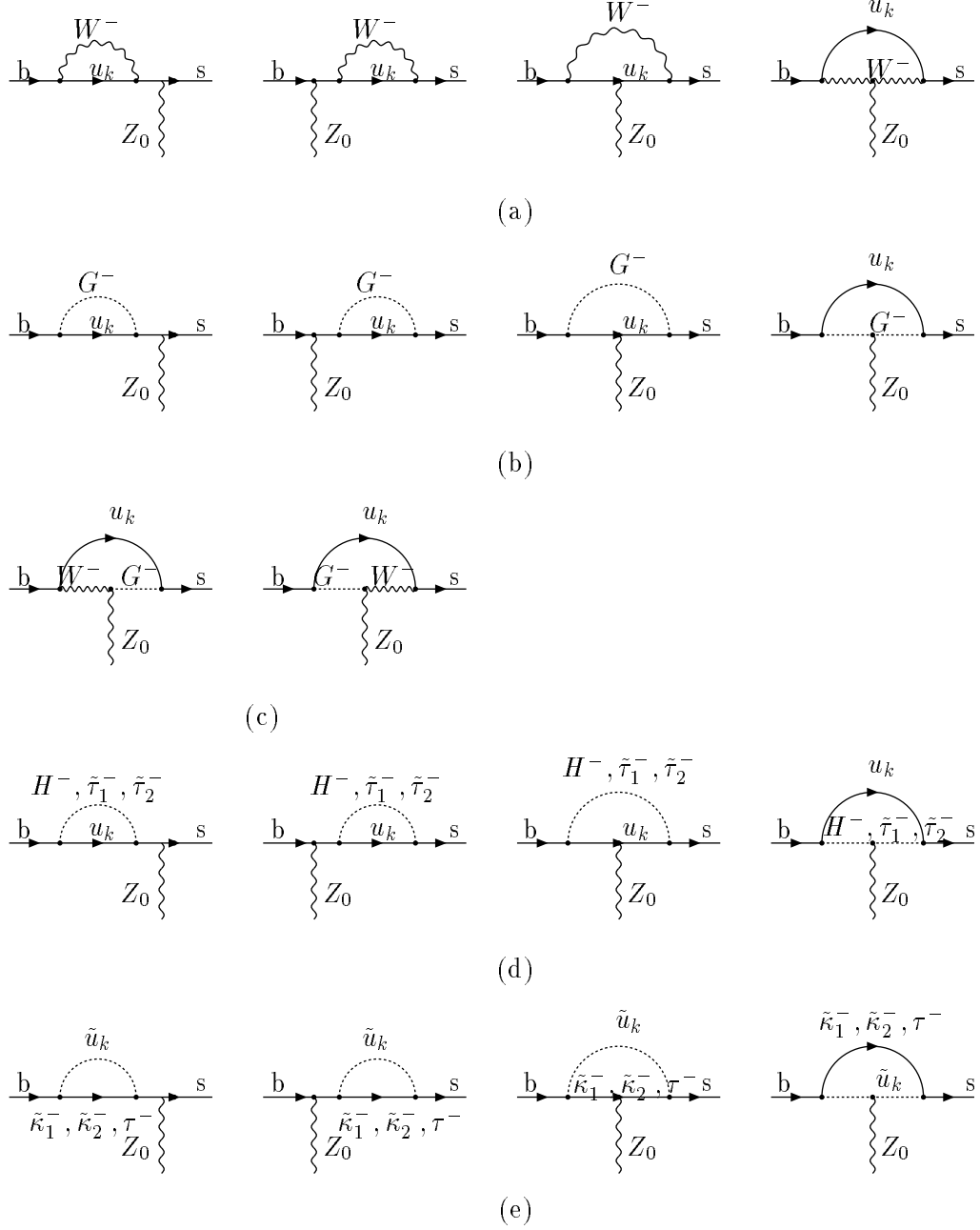


FIG. 1. The Feynman diagrams that contribute to bs and bsZ^0 coupling

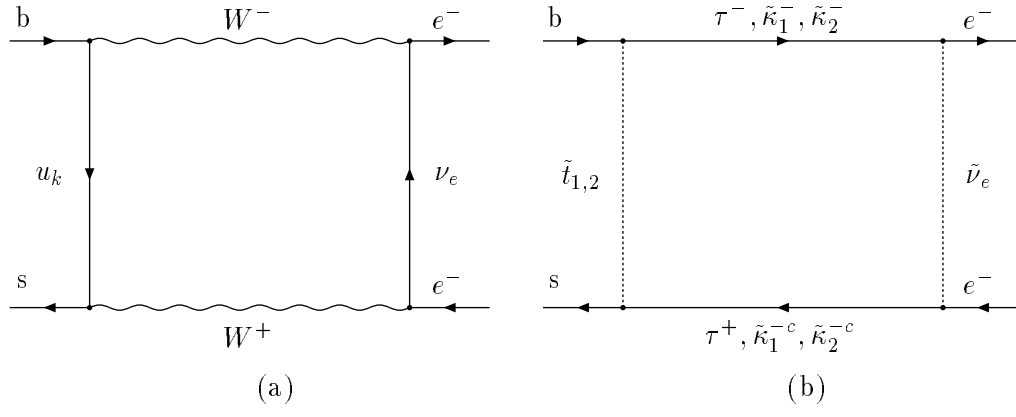


FIG . 2. The box diagrams contribute to $b \rightarrow s e^+ e^-$

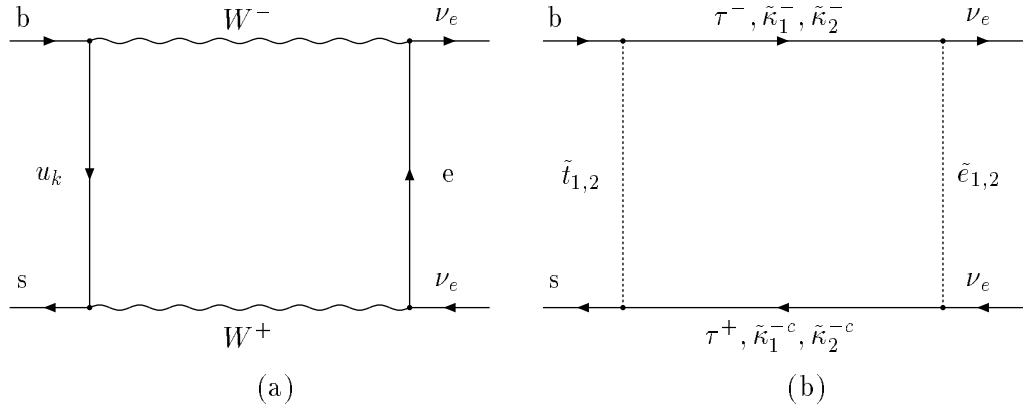


FIG . 3. The box diagrams contribute to $b \rightarrow s \nu_e \nu_e$

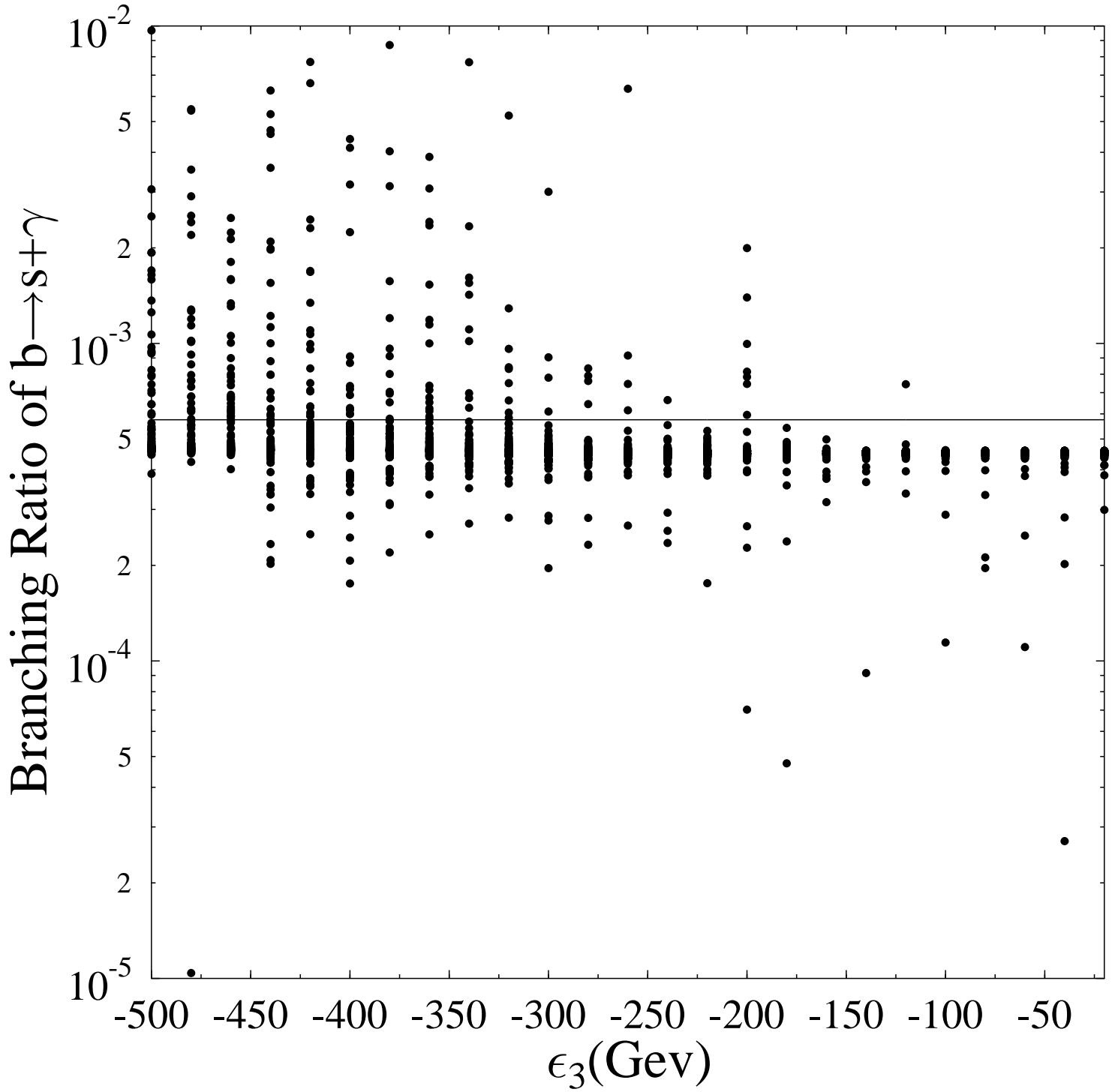


FIG . 4. The branching ration of $b \rightarrow s + \gamma$ vary with ϵ_3 when $\tan \beta = 20$, $\tan \beta = 40$; The solid-line is the prediction of SM .

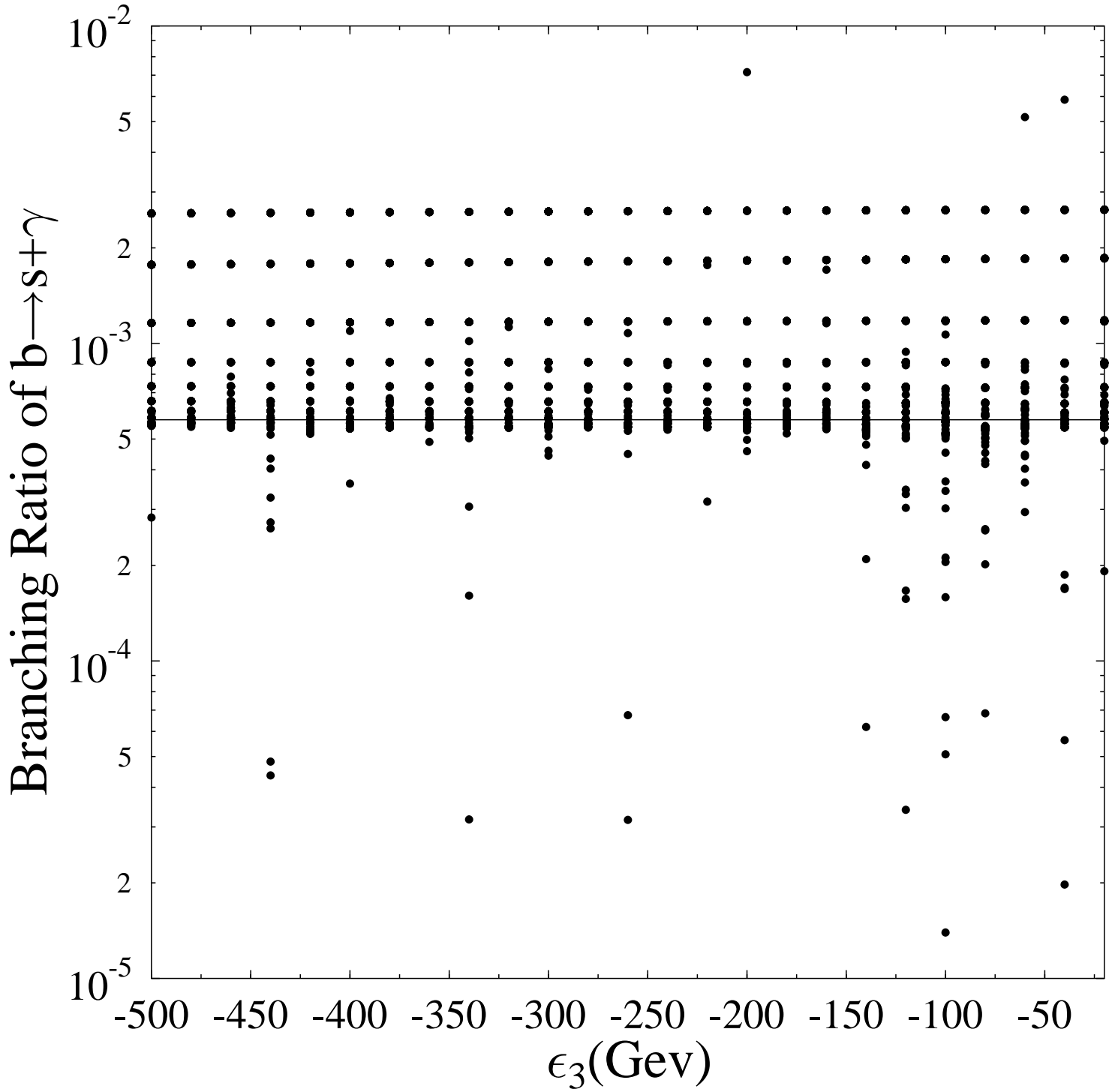


FIG . 5. The branching ration of $b \rightarrow s + \gamma$ vary with ϵ_3 when $\tan \beta = 2, \tan \beta = 40$;The solid-line is the prediction of SM .

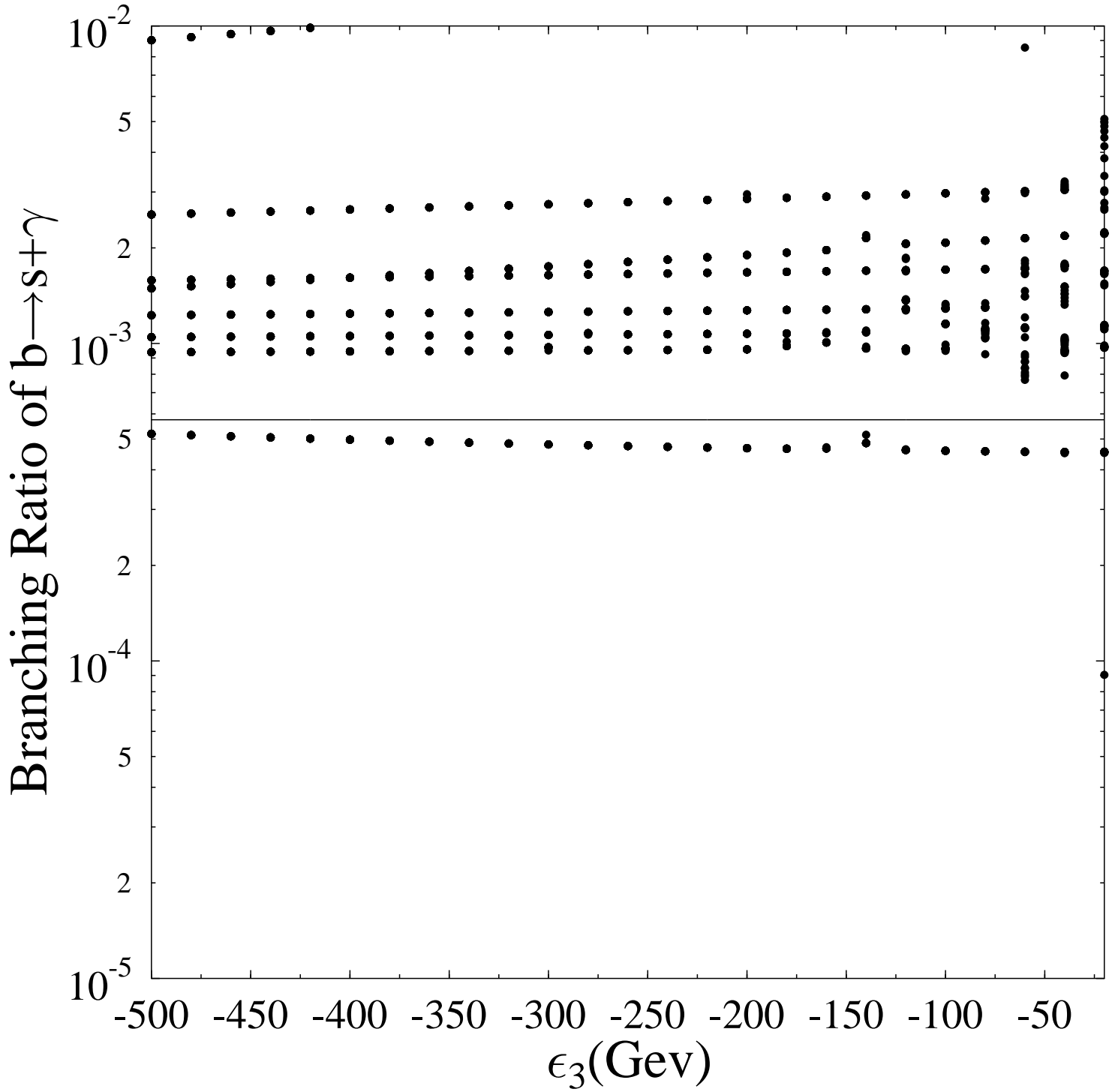


FIG . 6. The branching ration of $b \rightarrow s + \gamma$ vary with ϵ_3 when $\tan \beta = 0.5$, $\tan \beta = 40$; The solid-line is the prediction of SM .

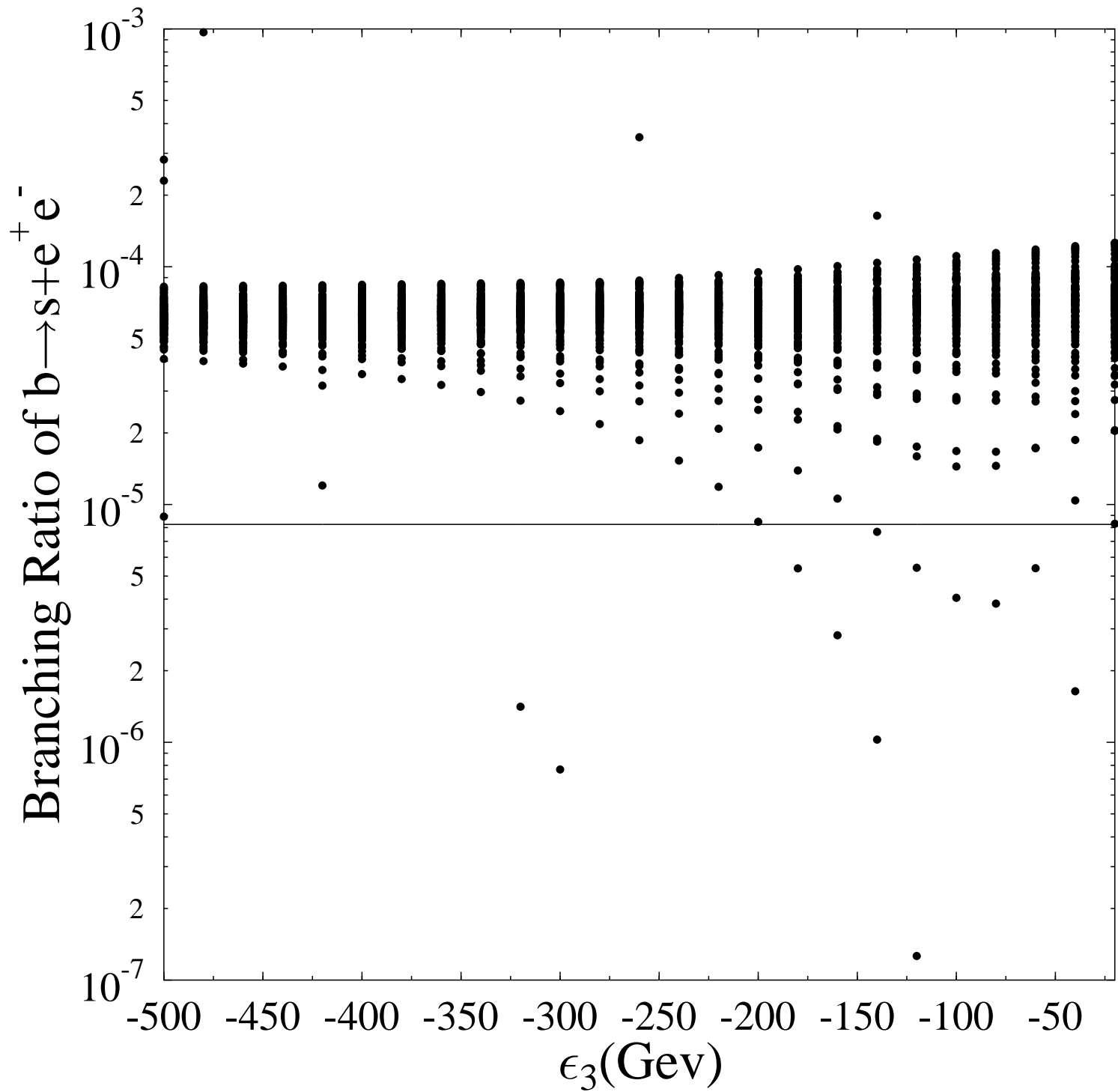


FIG .7. The branching ration of $b \rightarrow s + e^+ e^-$ vary with ϵ_3 when $\tan \beta = 20, \tan \beta = 40$; The solid-line is the prediction of SM .

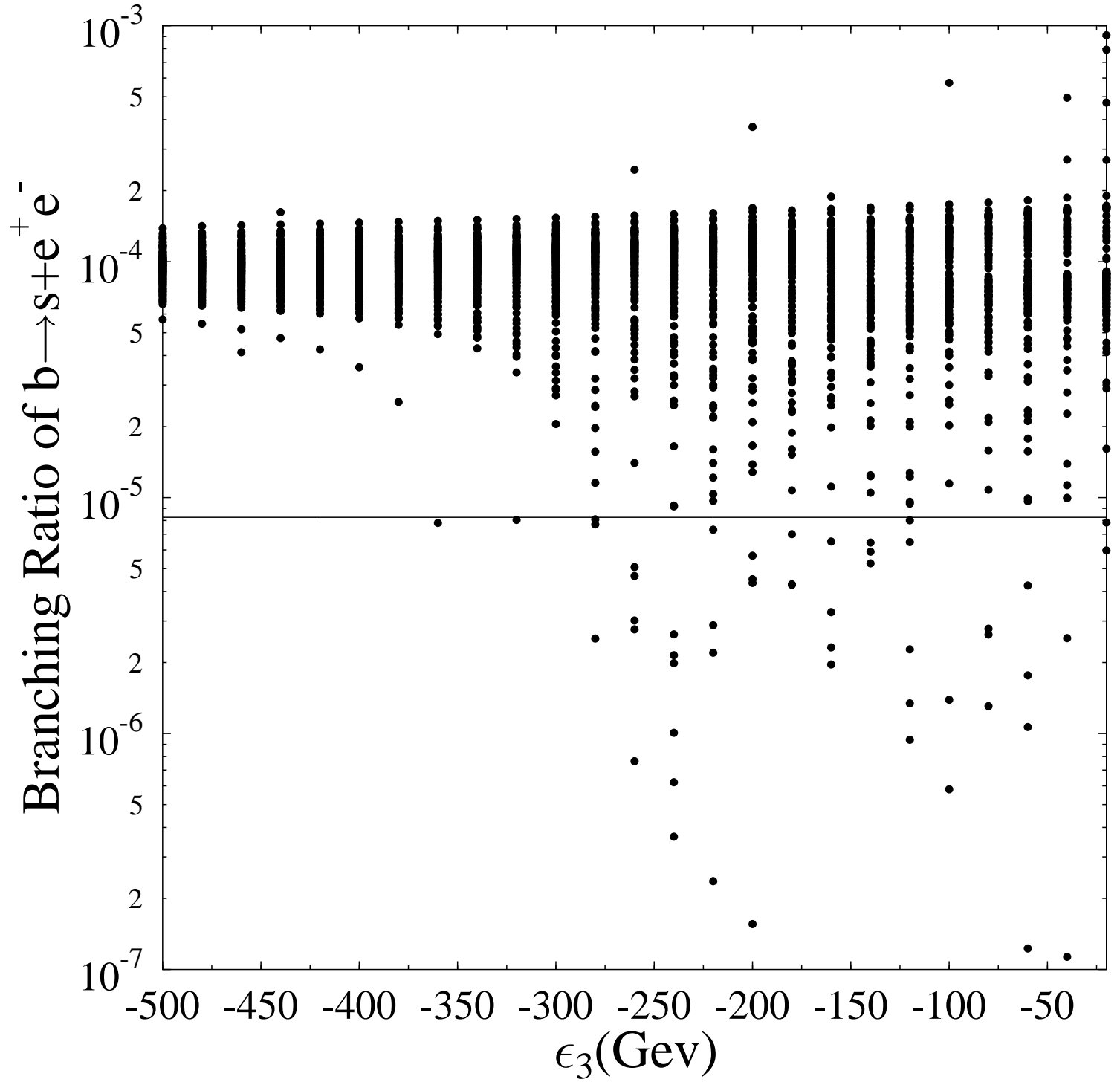


FIG .8. The branching ration of $b \rightarrow s + e^+ e^-$ vary with ϵ_3 when $\tan \beta = 2, \tan \beta = 40$; The solid-line is the prediction of SM .

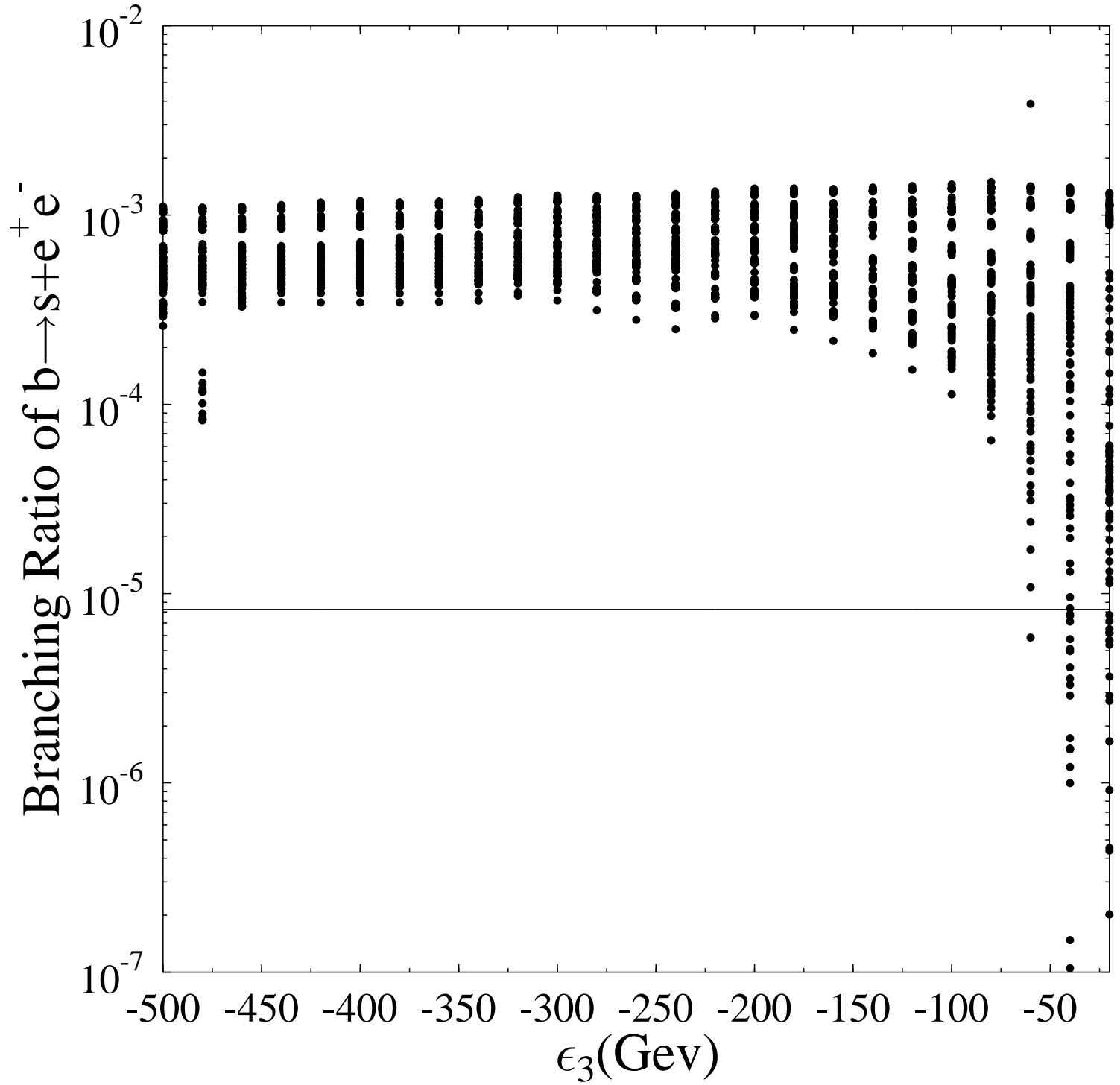


FIG .9. The branching ration of $b \rightarrow s + e^+ e^-$ vary with ϵ_3 when $\tan \beta = 0.5, \tan \beta = 40$; The solid-line is the prediction of SM .

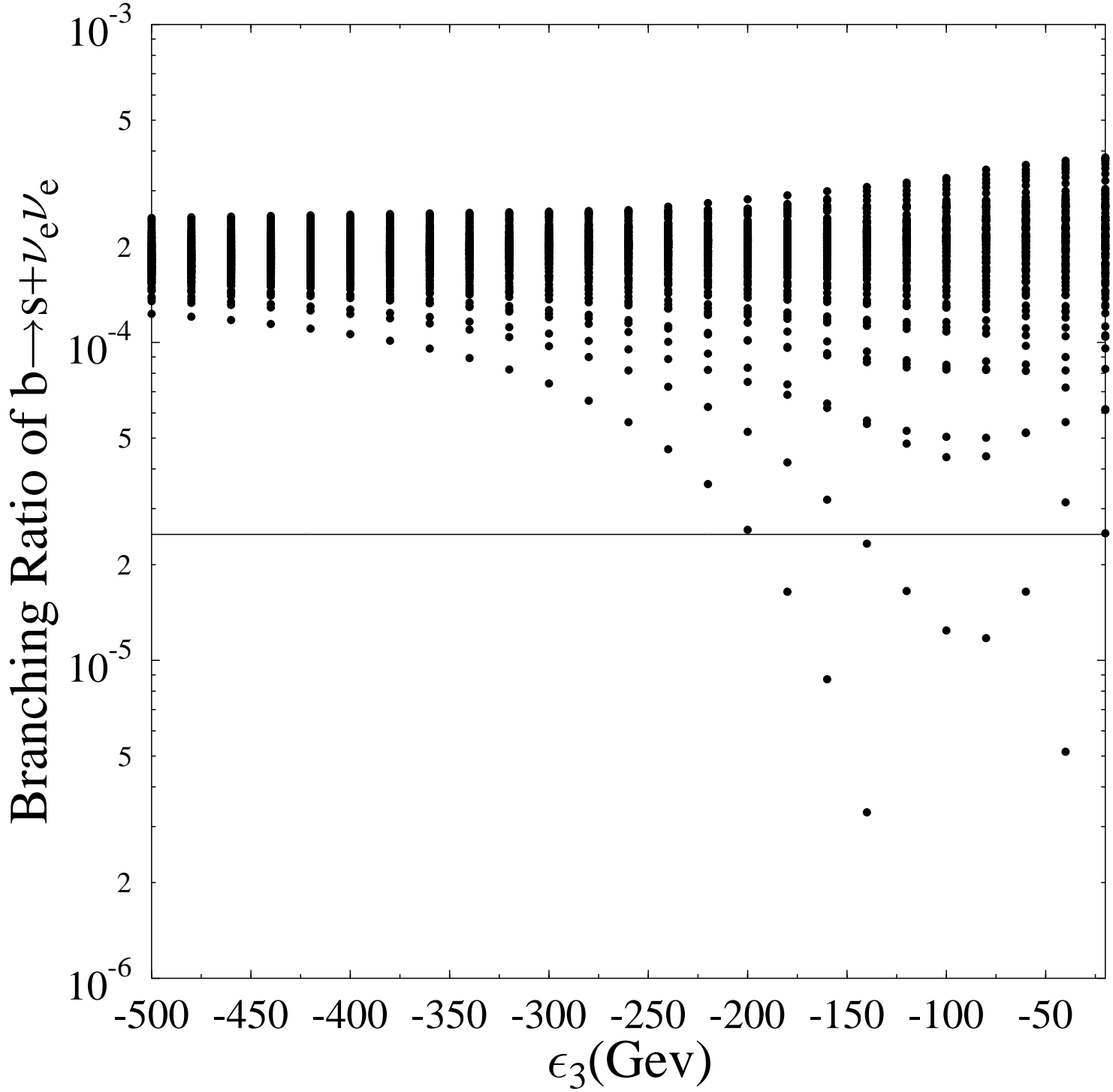


FIG .10. The branching ratio of $b \rightarrow s + \nu_e \nu_e$ vary with ϵ_3 when $\tan \beta = 20, \tan \beta = 40$; The solid-line is the prediction of SM .

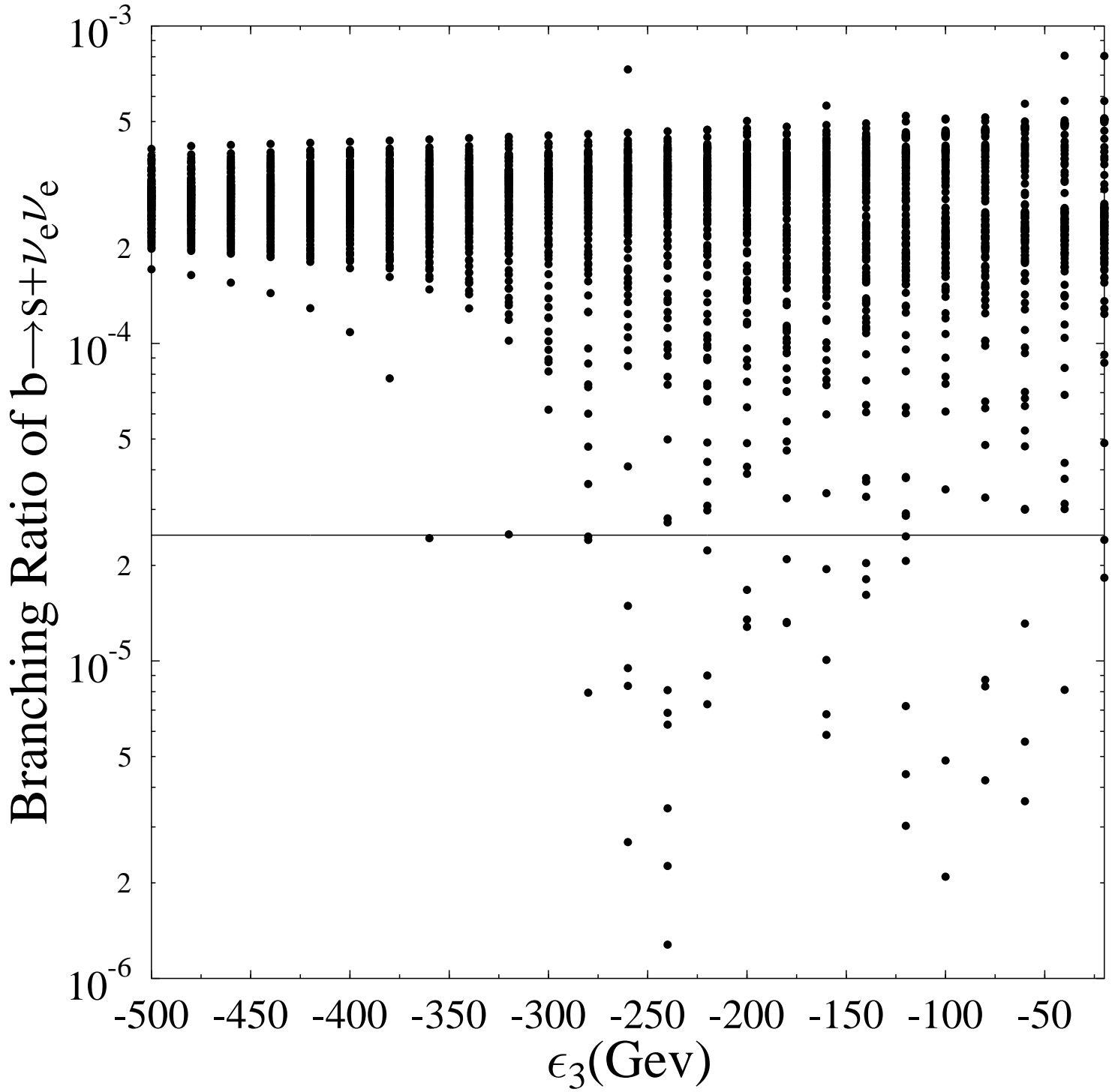


FIG .11. The branching ratio of $b \rightarrow s + \nu_e \bar{\nu}_e$ vary with ϵ_3 when $\tan \beta = 2, \tan \beta = 40$; The solid-line is the prediction of SM .

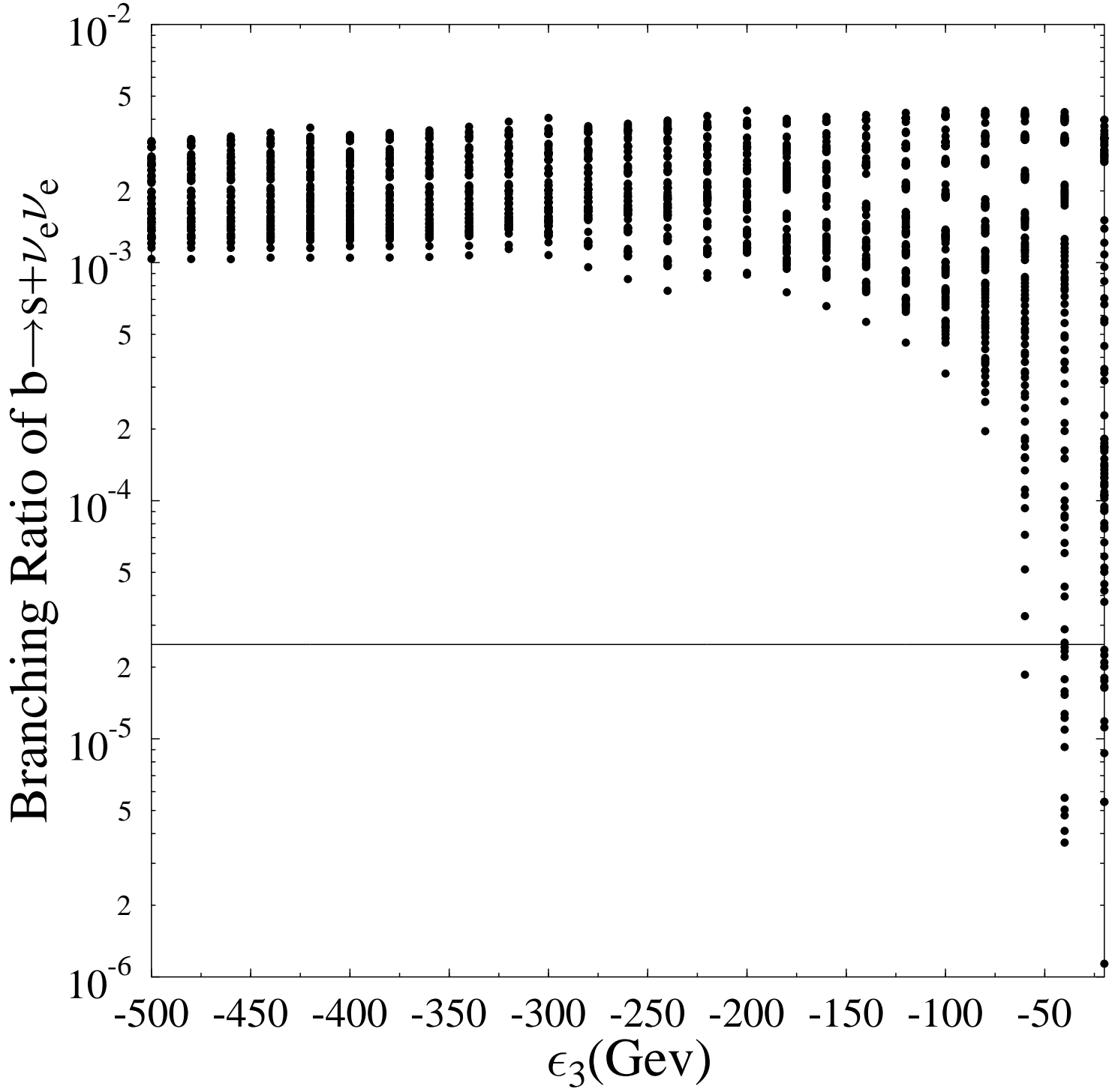


FIG .12. The branching ratio of $b \rightarrow s + \nu_e \nu_e$ vary with ϵ_3 when $\tan \beta = 5$, $\tan \beta = 40$; The solid-line is the prediction of SM .

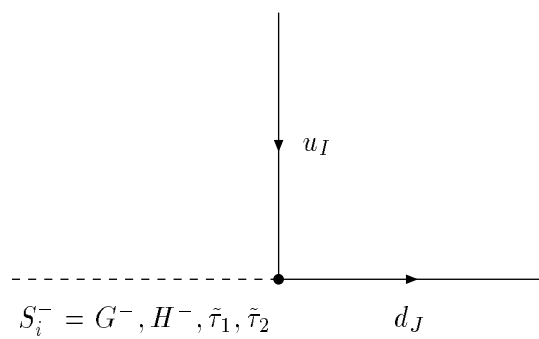


FIG .13. The coupling between $S_i = (G ; H ; \tilde{\tau}_1 ; \tilde{\tau}_1)$ and u_I, d_J

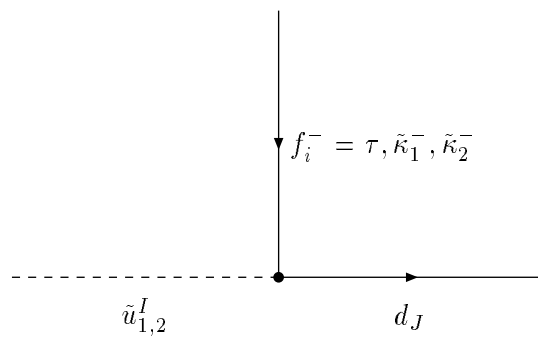


FIG .14. The coupling between $f_i = (; \sim_1 ; \sim_2)$ and d_J, α_j^I

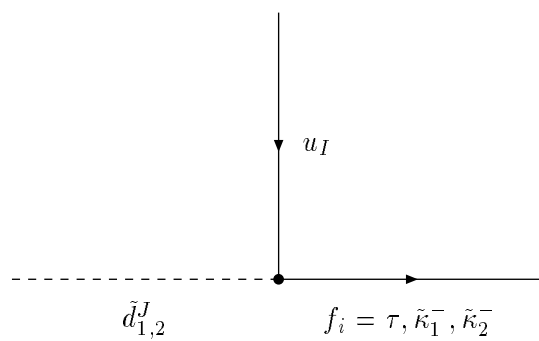


FIG .15. The coupling between $f_i = (; \sim_1 ; \sim_2)$ and u_I, \tilde{d}_j^J

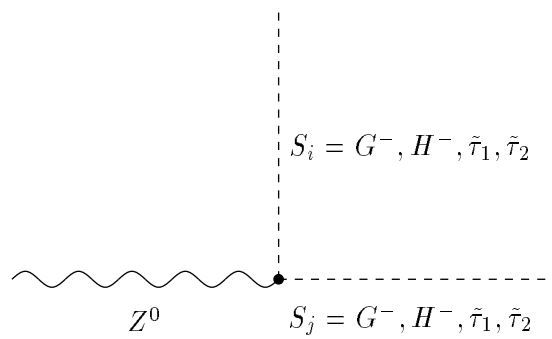


FIG .16. The coupling between Z^0 and $S_i = (G^-, H^-, \tilde{\tau}_1, \tilde{\tau}_2)$